Published in final edited form as:

J Am Chem Soc. 2023 May 31; 145(21): 11611–11621. doi:10.1021/jacs.3c01151.

Oligonucleotide Catabolism-Derived Gluconucleosides in *Caenorhabditis elegans*

Brian J. Curtis,
Boyce Thompson Institute and Department of Chemistry and Chemical Biology, Cornell University, Ithaca, New York 14853, United States

Tyler J. Schwertfeger,
Boyce Thompson Institute and Department of Chemistry and Chemical Biology, Cornell University, Ithaca, New York 14853, United States

Russell N. Burkhardt,
Boyce Thompson Institute and Department of Chemistry and Chemical Biology, Cornell University, Ithaca, New York 14853, United States

Bennett W. Fox,
Boyce Thompson Institute and Department of Chemistry and Chemical Biology, Cornell University, Ithaca, New York 14853, United States

Jude Andrzejewski,
Boyce Thompson Institute and Department of Chemistry and Chemical Biology, Cornell University, Ithaca, New York 14853, United States

Chester J. J. Wrobel,
Boyce Thompson Institute and Department of Chemistry and Chemical Biology, Cornell University, Ithaca, New York 14853, United States

Jingfang Yu,
Boyce Thompson Institute and Department of Chemistry and Chemical Biology, Cornell University, Ithaca, New York 14853, United States

Pedro R. Rodrigues,
Boyce Thompson Institute and Department of Chemistry and Chemical Biology, Cornell University, Ithaca, New York 14853, United States

Arnaud Tauffenberger,

Corresponding Authors: Arnaud Tauffenberger – Boyce Thompson Institute and Department of Chemistry and Chemical Biology, Cornell University, Ithaca, New York 14853, United States; at945@cornell.edu, **Frank C. Schroeder** – Boyce Thompson Institute and Department of Chemistry and Chemical Biology, Cornell University, Ithaca, New York 14853, United States; schroeder@cornell.edu.

Author Contributions

All authors have given approval to the final version of the manuscript.

Supporting Information

The Supporting Information is available free of charge at https://pubs.acs.org/doi/10.1021/jacs.3c01151.

General methods, bioassay procedures, methods for metabolomics, supporting schemes, synthetic procedures with NMR spectroscopic data, and NMR spectra (PDF)

Complete contact information is available at: https://pubs.acs.org/10.1021/jacs.3c01151

The authors declare the following competing financial interest(s): F.C.S. is a cofounder of Ascribe Bioscience and Holoclara Inc. The other authors declare no competing interests.

Boyce Thompson Institute and Department of Chemistry and Chemical Biology, Cornell University, Ithaca, New York 14853, United States;

Frank C. Schroeder
Boyce Thompson Institute and Department of Chemistry and Chemical Biology, Cornell University, Ithaca, New York 14853, United States;

Abstract

Nucleosides are essential cornerstones of life, and nucleoside derivatives and synthetic analogues have important biomedical applications. Correspondingly, production of non-canonical nucleoside derivatives in animal model systems is of particular interest. Here, we report the discovery of diverse glucose-based nucleosides in *Caenorhabditis elegans* and related nematodes. Using a mass spectrometric screen based on all-ion fragmentation in combination with total synthesis, we show that *C. elegans* selectively glucosylates a series of modified purines but not the canonical purine and pyrimidine bases. Analogous to ribonucleosides, the resulting gluconucleosides exist as phosphorylated and non-phosphorylated forms. The phosphorylated gluconucleosides can be additionally decorated with diverse acyl moieties from amino acid catabolism. Syntheses of representative variants, facilitated by a novel 2′-*O*- to 3′-*O*-dibenzyl phosphoryl transesterification reaction, demonstrated selective incorporation of different nucleobases and acyl moieties. Using stable-isotope labeling, we further show that gluconucleosides incorporate modified nucleobases derived from RNA and possibly DNA breakdown, revealing extensive recycling of oligonucleotide catabolites. Gluconucleosides are conserved in other nematodes, and biosynthesis of specific subsets is increased in germline mutants and during aging. Bioassays indicate that gluconucleosides may function in stress response pathways.

Graphical Abstract

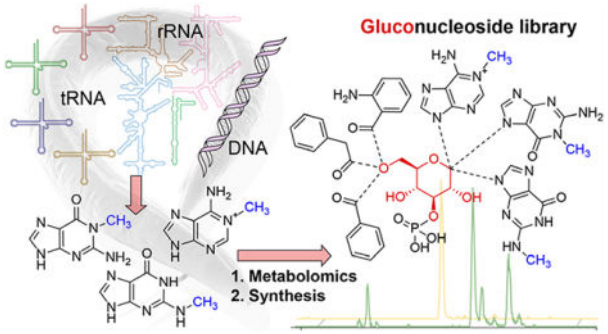

INTRODUCTION

Ribo- and deoxyribonucleotides are the building blocks of RNA and DNA, serve as ubiquitous chemical signals, and play essential roles in intracellular energy transfer. Correspondingly, nucleoside derivatives obtained from natural sources as well as synthetic analogues are of great interest for biomedical research, and nucleoside analogues represent a major class of antiviral and anticancer drugs.[1,2] For example, the 2′-fluoronucleoside analogue sofosbuvir, an FDA-approved hepatitis C drug, also has the potential to inhibit

replication of SARS-CoV-2 in cell culture.[3] Surprisingly, nucleoside metabolism in animal model systems has not been investigated using state-of-the-art untargeted metabolomics and high-resolution mass spectrometry (HRMS), which greatly facilitate the identification of cryptic chemotypes. Identification of nucleoside derivatives from animal sources may reveal new aspects of nucleoside function and may provide valuable new leads for drug development.

Signaling networks in the model organism *Caenorhabditis elegans* and other nematode species have revealed a few cases in which pentose-based nucleosides possibly derived from RNA breakdown are attached to glycosides derived from the 3,6-dideoxysugars ascarylose and paratose.[4–6] Examples include the ascaroside, nuclas#31 (**1**),[4] from *C. elegans*, which incorporates N^6, N^6-dimethyladenosine (m6,6,A), as well as npar#1 (**2**), a paratoside from the satellite model *Pristionchus pacificus*.[5] Uniquely, the structure of npar#1 includes an N^6-threonylcarbamoyladenine-based D-xylopyranose, instead of the canonical D-ribofuranose. npar#1 functions as an inter-organismal signal that potently triggers arrest of larval development at the dauer stage, demonstrating the biological significance of nucleoside-derived natural products in nematodes.[5]

In addition to pentose-based nucleosides, recent studies revealed the presence of unusual hexose-based nucleosides in *C. elegans*. These include pugl#1 (**3**), featuring N^6-isopentenyl-2-methylthioadenine linked via the N^9-position to β-glucopyranose[4] and the uglas-family glucosides, e.g., uglas#11 (**4**), representing an N^3-linked uric acid β-glucopyranoside that is acylated and phosphorylated in positions 2′ and 3′ of the glucopyranose, respectively (Figure 1).[6] Notably, glucosylation of modified adenines also plays an important role in plant biology. Examples include (*E*)-zeatin and kinetin glucosides (**5** and **6**, respectively), which belong to the cytokinin family of plant hormones.[7] Cytokinins control many aspects of plant growth and development, and their activity is regulated in part via glucosylation at the N^9- or N^7-positions on the adenine moieties.[8]

Based on the biological significance and biomedical potential of nucleoside derivatives, we set out to survey the *C. elegans* metabolome for the presence of non-canonical nucleosides. Whereas the above examples were discovered serendipitously while pursuing biological phenotypes lacking any obvious connection to nucleoside metabolism, we here develop a targeted approach using a combination of several mass spectrometric (MS) approaches and synthesis. Following identification of several series of gluconucleosides, we then employ stable-isotope labeling to demonstrate their likely origin from RNA catabolism and investigate conservation of gluconucleoside production across different species. In addition, we consider factors that affect gluconucleoside production.

RESULTS

Free Nucleobases in the *C. elegans* Metabolome.

Although little is known about the biosynthesis of non-ribose-based nucleosides in nematodes, it seemed likely that the previously identified gluco- and xylonucleosides are derived from glycosylation of free nucleobases originating from RNA and DNA catabolism.[9] For example, npar#1 incorporates a highly modified adenine conceivably

derived from tRNA breakdown.[5] To assess the extent to which diverse modified or unmodified nucleobases are available for potential incorporation into secondary metabolic pathways in *C. elegans*, we first surveyed the *C. elegans exo*- and *endo*-metabolomes for the presence of known modified nucleobases, in addition to the canonical adenine, guanine, cytosine, uracil, and thymine. Targeted analysis via HPLC, coupled to HRMS, for known nucleobases revealed the presence of large quantities of methylated purines, most prominently N^1-methyladenine (**7**), N^1- and N^2-methylguanine (**9** and **10**), as well as N^2, N^2-dimethylguanine (**11**), in addition to the canonical bases (Figures 2a and S1, Table S1). Xanthine, N^6-isopentenyl-2-methylthioadenine, and threonylcarbamoyladenine (t6A) were also detected.

All-Ion Fragmentation (AIF) Reveals Non-Canonical Methylpurine Metabolites.

To assess if and to what extent the identified free nucleobases are integrated into other metabolites, e.g., non-canonical nucleosides, we employed HPLC−HRMS analyses in AIF mode. In AIF mode, also referred to as MS^E or MS/MS^{ALL}, the analyte is continuously and indiscriminately (without prior ion selection) fragmented, which enables screening metabolome samples for specific product ions across the entire retention time/polarity range.[10–12] Applied to nucleosides, AIF takes advantage of the relative resilience of the nucleobase cores toward additional fragmentation and their facile ionization in ESI^+ mode. To obtain a comprehensive overview of potentially nucleobase-incorporating metabolites, we conducted AIF analyses of *C. elegans endo*- and *exo*-metabolome samples using both reversed-phase (C18) and hydrophilic interaction liquid chromatography (HILIC) chromatography, providing coverage of metabolites from a wide polarity range (Figure 2b,c). These analyses revealed an unexpectedly large number of compounds, primarily in the *endo*-metabolome, that produced fragment ions indicative of incorporation of modified nucleobases. Manual curation of the corresponding MS^2 data revealed a large number of putative derivatives of methylated adenine and guanine as well as dimethylguanine. In contrast, few peaks were observed that featured fragments derived from the unmodified five canonical nucleobases (e.g., adenine and guanine, Figure 2c).

The MS^2 spectra of the putative methylpurine-containing peaks detected via AIF suggested that they belong to two distinct metabolite families, (i) simple hexose-based nucleosides and corresponding phosphates and (ii) larger structures in which the hexosylated nucleobases were combined with building blocks from other metabolic pathways (Figure 2d,e, Tables S2 and S3). In total, we detected putative hexosylated derivatives of several different modified purine bases and ~30 more complex metabolites representing hexosylated nucleosides bearing additional acyl moieties, most of which appeared to be derived from amino acid catabolism (e.g., phenylacetyl, anthranoyl, nicotinoyl, etc., Figure 2e). Conversely, AIF peaks for the canonical nucleobases were found to represent the corresponding ribo- or deoxyribonucleosides and their corresponding phosphates; hexosylated derivatives were not detected, indicating that hexosylation is selective for modified purines (Figure S2). We next asked whether the hexose-based nucleosides could originate from the *Escherichia coli* bacteria that are used as food for growing *C. elegans*. However, none of the putative non-canonical nucleoside derivatives were detected in *E. coli* extracts, suggesting that they are products of *C. elegans* metabolism.

Identification of Glucosylated Methylpurines.

While the previous identification of the gluconucleoside pugl#1 (**3**) suggested that the hexosylated purines represent glucosides, establishing their exact identities was non-trivial, given the presence of several different methyladenine and methylguanine isomers and since some purine bases can be glycosylated at different positions.[13,14] Therefore, we developed a flexible synthetic approach that would provide access to diverse structural variants, which then could be compared with the natural isomers via retention times and MS^2 (Figure 3). We first focused on methyladenine derivatives, one of the most abundant nucleobase-derived metabolite families. HPLC−MS^2 analysis revealed one major peak for a putative methyladenine glucoside, in addition to trace amounts of potential isomers. Since we detected both N^1- and N^6-methyladenine in our initial metabolomic analysis, we synthesized the corresponding N^9-β-linked glucosides,[15] of which the N^1-isomer (maglu#1, **13**) was identified as the major natural isomer (Figure 3a), based on comparison of MS^2 spectra and retention times (Figures S3 and S4). In addition, we detected trace amounts of N^6-methyladenine glucoside (maglu#3, **14**) (Figures 3a and S4), reflecting the much lower abundance of free N^6-methyladenine relative to the N^1-isomer.

For putative methylguanine glucosides, our metabolomic analyses revealed at least three isomers of roughly similar abundance (Figure 3b). Since our nucleobase screen had revealed N^1-, N^2-, and N^7-methylguanine, we synthesized the corresponding N^9-β-glucosides as well as the N^7-β-glucoside of N^1-methylguanine via Vorbrüggen conditions[16] using appropriate purine base precursors (Scheme S1). As in the case of the methyladenine derivatives, we used MS^2 spectra and multiple chromatographic conditions to establish the identities of the naturally occurring isomers. We found that the N^9-β-glucosides of N^1- and N^2-methylguanine (mgglu#1, **15** and mgglu#3, **18**) co-eluted with the less abundant natural isomers (Figures 3b, S5, and S6), whereas the major natural isomer was identified as N^1-methyl-N^7-glucosylguanine (mgglu#5, **16**, Figure S5). In contrast, N^7-methyl-N^9-glucosylguanine did not co-elute with any of the natural isomers, even though free N^7-methylguanine is similarly abundant as its isomers (Figures S1 and S6).

Finally, we targeted the putative dimethylguanine glucoside isomers, which we assumed to be derived from N^2, N^2-dimethylguanine as the only purine observed in the metabolome samples (Figures 2a, 3c, and S1). Both the N^9- and N^7-glucosylated isomers were synthesized using a $SnCl_4$-mediated coupling of 2,6-dichloropurine and peracetylated glucose for preparation of the N^7-isomer (Figure 3b,c).[17] Comparison of MS^2 spectra and retention times indicated that *C. elegans* produces primarily N^2, N^2-dimethyl-N^7-β-glucosylguanine (dmgglu#3, **21**, Figure S7), in addition to smaller amounts of the corresponding N^9-glucosylated isomer, dmgglu#1 (**19**).

Synthesis of Phosphorylated Derivatives via 2′-*O*- to 3′-*O*-Transphosphorylation.

Having established the identities of the non-phosphorylated glucosides, we next pursued their corresponding phosphates. These were assumed to represent the 3′-*O*-phosphorylated isomers, in analogy to uglas#11 (**4**) and other phosphorylated glucosides recently identified in *C. elegans*.[6,18–21] Toward selective installation of a 3′-*O*-phosphate in N^1-methyladenine glucoside (maglu#1, **13**), we first protected the 4′-*O*- and 6′-*O*-positions

of N^9-glucosyladenine (**22**) using $TIPDSiCl_2$ (Figure 4a). To introduce a 3′-*O*-phosphate ester moiety, we originally planned to employ selective 2′-*O*-protection with carboxybenzyl (Cbz);[21] however, subsequent dibenzyl phosphorylation, using a $P(OBn)_2N(iPr)_2$/mCPBA addition/oxidation sequence, was difficult to control, and it produced significant amounts of *N*-phosphorylated side products even in the presence of ImOTf.[22,23]

Therefore, we opted for phosphorylation of the 2′-*O*-unprotected **23**, which resulted in reduced *N*-phosphorylation but produced predominantly the 2′-*O*-phosphate, in addition to smaller amounts of the desired 3′-*O*-phosphate. Gratifyingly, we found that subsequent treatment with TBAF for silyl deprotection additionally promoted 2′-*O*- to 3′-*O*-migration of the phosphate moiety[24] (Figures S8 and S9, Table S4), producing the 3′-*O*-phosphorylated **24** as the predominant isomer, from which small residual amounts of the corresponding 2′-*O*-isomer could be easily separated. N^1-methylation of 3′-*O*-isomer **24** followed by Pd/C-catalyzed hydrogenation under basic conditions[25] furnished maglu#2 (**25**), whose HPLC retention times and MS^2 spectra were identical to those of the natural isomer (Figures 4d and S10).

Use of the TBAF-mediated 2′-*O*- to 3′-*O*-transphosphorylation strategy simplified synthesis of the other proposed gluconucleoside phosphates, including the N^9- and N^7-glucosylated derivatives of N^1-methylguanine [mgglu#2 (**31**) and mgglu#6 (**30**), Figures 4b and S9]. TBAF treatment yielded generally 65−70% of the 3′-*O*-phosphorylated species from starting materials that consisted predominantly (~95%) of the 2′-*O*-phosphorylated isomers. Comparison of retention times of mgglu#2 (**31**) and mgglu#6 (**30**) with the corresponding peaks in the *C. elegans* metabolome confirmed the proposed structures, consistent with glucosylation patterns of the non-phosphorylated derivatives **15** and **16** (Figures 4c and S11).

C. elegans Produce Diverse 6′-*O*-Acylated Gluconucleosides.

For identification of the putative acylated gluconucleoside derivatives, we considered that in nematodes, 2′-*O*- and/or 6′-*O*-acylation of diverse 3′-*O*-phosphorylated glucosides was recently shown to be mediated by a family of carboxylesterase (*cest*) homologues, whereby 2′-*O*-acylated derivatives are generally observed at earlier retention times than the corresponding 6′-*O*-acylated isomers.[19,20] Since almost all so-far characterized 2′-*O*-acylated glucosides require CEST-1.1 or CEST-1.2, we first assessed whether the abundances of acylated gluconucleosides were affected in *cest-1.1* and *cest-1.2* mutants. We found that minor earlier eluting isomers of acylated methylguanine derivatives were abolished in *cest-1.2* mutants, suggesting that most of the detected acylated gluconucleosides represent 6′-*O*-acylated derivatives (Figure 5a, Table S3).

To confirm these assignments, we targeted one of the most abundant families of acylated gluconucleosides, representing putative phenylacetyl derivatives, starting from dibenzyl phosphate precursors (**24**, **28**, and **29**). Acylation with phenylacetic acid using TBTU/pyr[26,27] afforded the corresponding 6′-*O*-phenylacetylated derivatives (**32**–**34**) with high selectivity (Figure 5b). Methylation of adenine derivative **32** followed by Pd/C hydrogenation under basic conditions afforded maglu#11 (**35**), whose identity as the

naturally produced isomer was confirmed via HPLC retention times and MS^2 spectra (Figures 5c and S12). Similarly, deprotection of N^7- and N^9-linked N^1-methylguanine derivatives **33** and **34** afforded mgglu#51 (**36**) and mgglu#11 (**37**), with the N^7-glucosylated derivative **36** representing the more abundant natural isomer (Figures 5d and S13). Given that we had also identified N^2-methylguanine glucoside (**18**), we additionally synthesized the corresponding 6′-*O*-phenylacetyl 3′-*O*-phosphate **39** (Figures 5b,d, and S16, Scheme S2);[21] however, this compound did not correspond to any of the natural isomers, demonstrating a high level of selectivity in the biosynthesis of these acylated gluconucleosides. To further investigate selectivity of the assembly of acylated methylguanine-derived gluconucleosides, we also synthesized the 6′-*O*-benzoylated derivative of N^7-glucosylated N^1-methylguanine (mgglu#52, Figures S14 and S15), which, like the related phenylacetyl derivative, was found as the major isomer of the corresponding series of AIF-detected isobaric gluconucleosides. These results suggested that major isomers of the remaining acylated gluconucleosides represent 6′-*O*-acylated derivatives of N^7-glucosylated-N^1-methylguanine and N^9-glucosylated-N^1-methyladenine (see Figures S17 and S18 for chromatograms and proposed structures).

Gluconucleoside Profiles Are Species-Specific.

Next, we investigated whether gluconucleoside biosynthesis is conserved in other nematode species. We found that the closely related species, *C. briggsae*, produces an overall similar profile of gluconucleosides; however, relative abundances of isomers differed significantly between the two *Caenorhabditis* species (Figure S17). For example, *C. briggsae* produces the phenylacetyl derivative of N^9-glucosylated N^2-methylguanine (**39**, mgglu#31), which is absent in *C. elegans*, in addition to smaller amounts of the N^7-glucosylated N^1-methylguanine derivative **36**, which is the major isomer in *C. elegans* (Figure 5d). Abundances of isomers of other acylated methylguanine derivatives (anthranoyl, benzoyl, etc.) show similar differences between *C. briggsae* and *C. elegans* (Table S5, Figure S17). In another example, *C. briggsae* produces only the later-eluting N^9-glucosylated isomer of N^2, N^2-dimethylguanine, dmgglu#1 (**19**), whereas the N^7-glucosylated variant (dmgglu#3, **21**), the major isomer in *C. elegans*, is absent (Figure S19).

Furthermore, we surveyed the metabolome of *P. pacificus*,[28] a nematode species that has been established as a more distantly related “satellite” model system to *C. elegans*. Like *C. elegans* and *C. briggsae*, *P. pacificus* also produces N^1-methyladenine glucoside (maglu#1, **13**) and the corresponding phosphate (maglu#2, **25**, Figure S20). In contrast, most other gluconucleosides identified from the two *Caenorhabditis* species could not be detected in *P. pacificus*, including all annotated methylguanine derivatives (Figure S21), except for N^6, N^6-dimethyl-N^9-glucosyladenine (dmaglu#1, **19**), which was detected in all three analyzed species (Figure S22). Additionally, several acylated N^6, N^6-dimethyladenine-containing glucosides were detected in the *P. pacificus endo*-metabolome, which were not observed in *C. elegans* or *C. briggsae* (Figure S23). Taken together, these analyses demonstrate that among the tested species, gluconucleoside production is generally conserved, but compound profiles differ between species.

Assessing the Origin of Methylated Gluconucleosides.

Our AIF-based analysis of the *C. elegans* metabolome revealed diverse putative methyladenine and methylguanine glucosides whose structures we subsequently confirmed via synthesis. In contrast, we did not detect any glucosides of unmodified adenine or guanine (Figures 2c and S2), even though free adenine and guanine are highly abundant (Figure 2a), suggesting that the identified gluconucleosides originate from glucosylation of RNA breakdown-derived methylpurine substrates, instead of methylation of adenine or guanine glucosides. To further support a possible RNA origin of the modified purines, we isolated and enzymatically hydrolyzed *C. elegans* and *C. briggsae* total RNA. HPLC−MS analysis of hydrolyzed RNA revealed both N^1- and N^6-methyladenosine as well as several methylguanosine isomers, including N^1-, N^2-, and N^7-methylguanosine,[29] similar to the observed profile of free nucleobases in the *endo*-metabolome (Figure S24). Next, we supplemented synchronized *C. elegans* cultures with CH_3-or CD_3-N^1-methyladenine (**7** and **40**) until reaching sexual maturity (Figure 6a). HPLC−HRMS analysis of the *endo*-metabolome of methyladenine-supplemented animals revealed extensive incorporation of the CD_3 label into N^1-methyladenine glucoside (**41**) and its derivatives (Figure S25). These results are consistent with a model in which modified purines derived from RNA and/or DNA catabolism are repurposed for the biosynthesis of gluconucleoside derivatives. Interestingly, we also observed a smaller amount of incorporation of the CD_3 label into N^1-methyl*ribo*adenosine (Figure S26); however, no incorporation was observed in N^1-methylriboadenosine derived from hydrolyzed RNA (Figure S27), consistent with the canonical origin of N^1-methylriboadenosine from methylation of RNA and DNA.

Gluconucleoside Production Is Age- and Sex-Dependent.

Next, we considered the biological conditions that may influence production of the methylpurine-derived gluconucleosides. Methylation in DNA and RNA serves as a biomarker for various diseases as well as aging and plays important roles during gametogenesis in the germline.[31–34] First, we profiled gluconucleoside production during development, at different larval stages, as well as during early and late adulthood. Overall, gluconucleoside production remained low during development and increased significantly after reaching sexual maturity and increased further in aged adults (Figures 6b, S28, and S29). The levels of the corresponding non-glycosylated methylpurines also increased throughout development and aging, though less dramatically (Figure S29). Next, we investigated a series of germline mutants and found that production of two gluconucleoside derivatives bearing a phenylacetyl moiety, maglu#11 (**35**) and mgglu#51 (**36**), was greatly increased in animals with a masculinized germline (Figures 6b and S30),[30] whereas levels of the unmodified gluconucleoside, maglu#2 (**25**), were largely unchanged in masculinized animals. It thus appears that production of the phenylacetylated maglu#11 and mgglu#51 is specifically associated with the presence of a male germline. Finally, we found that production of acylated gluconucleosides was generally increased under starvation conditions, possibly as a result of increased RNA degradation in response to reduced nutrient levels (Figure S31).[35] The strong increase of gluconucleoside production during aging and starvation suggested that gluconucleoside production may be part of organismal stress responses. To investigate this idea, we selected maglu#1 (**13**), which is produced by

all three species analyzed in this study, for a bioassay that measures resistance to juglone-induced oxidative stress[36] (Figures 6c and S32). Preconditioning of animals for 24 h with maglu#1 (**13**) resulted in significantly increased survival following juglone exposure. More detailed analyses are needed to investigate the underlying mechanisms; however, these initial results indicate that maglu#1 (**13**) may prime or activate stress response pathways.

DISCUSSION

Our AIF-guided metabolomic analyses revealed an unexpected facet of nucleoside metabolism in *C. elegans*: a wide range of methylpurine-derived gluconucleosides, corresponding phosphates, and additionally acylated variants. In contrast to many other metabolites identified from *C. elegans*, e.g., the ascarosides, which serve as inter-organismal signals, the gluconucleosides and especially their phosphorylated variants are mostly retained in the *endo*-metabolomes, suggesting a role in intra-organismal processes. Phosphorylated methylpurine glucosides are structurally similar to *ribo*adenosine and *ribo*guanosine phosphates and their cyclic derivatives, which are of central importance as second messengers involved in almost every aspect of intra- and intercellular signaling.[37] Although a detailed functional evaluation of gluconucleosides is beyond the scope of this study, our preliminary survey of conditions associated with gluconucleoside production suggests distinct biological contexts for the identified gluconucleoside variants; for example, the phenylacetyl derivatives **35** and **36** are specifically associated with the male germline, whereas non-acylated variants are produced upon reaching reproductive maturity independent of sex. Furthermore, we found that gluconucleoside production is strongly induced upon aging and during starvation, suggesting that they may play a role in modulating purinergic signaling in stress response pathways. Consistent with this idea, pretreatment with maglu#1 (**13**) increased oxidative stress resistance, providing a starting point for the biological roles of gluconucleosides.

Interestingly, all identified gluconucleoside variants incorporate modified nucleobases, whereas unmodified glucoadenosine or glucoguanosine was undetectable in *C. elegans*, despite free adenine and guanine being highly abundant in the *endo*-metabolomes. This suggests that gluconucleosides are produced selectively from a subset of free nucleobases, as also supported by the incorporation of stable-isotope-labeled N^1-methyladenine into N^1-methylglucoadenosines (Figure 6a). The modified nucleobases in the gluconucleosides all represent known RNA and DNA modifications, and we confirmed that *C. elegans* and *C. briggsae* RNA does contain the corresponding ribonucleosides. Therefore, it appears that the nucleobase pool used for gluconucleoside production is derived from RNA and DNA catabolism (Figure 6d). Likely, both nematode and bacterial oligonucleotide catabolism contribute since methylpurines were abundant in *E. coli* extracts and, as we showed, can be incorporated when externally applied. Curiously, we also observed incorporation of stable-isotope-labeled N^1-methyladenine into N^1-methyl*ribo*adenosine, indicating that whereas glucosylation is specific for modified nucleobases, ribosylation may be less selective. Stable-isotope-labeled N^1-methylriboadenosine was not detected in hydrolyzed total RNA, consistent with post-transcriptional base methylation, and thus, the production of N^1-methylriboadenosine suggests that modified ribonucleosides may have other roles beyond representing intermediates of nucleic acid catabolism.

The identified gluconucleosides are all based on modified purine bases that are particularly abundant in tRNA and rRNA. Notably, tRNA and rRNA degradation represents a conserved stress response,[38–40] and fragments resulting from tRNA breakdown (tRFs) have been shown to serve diverse cellular functions.[41–43] Our finding that maglu#1, based on primarily tRNA- and rRNA-derived N^1-methyladenine, promotes stress resistance suggests that gluconucleoside production may represent another layer of stress-induced metabolic changes that, like tRFs, contributes to the activation of stress resistance pathways.

Highly regioselective glucosylation of modified purines suggests involvement of dedicated glucuronosyltransferases (UGTs) or other glycosylation enzymes (Figure 6d), similar to the putative biosynthesis of cytokinin glucosides in *Arabidopsis* and other plants.[44,45] Subsequent 6′-*O*-acylation of the resulting gluconucleosides may involve members of the *cest* family of carboxylesterases, which have been recently shown to mediate attachment of diverse acyl moieties to structurally similar glucosides.[19,20,46] For example, 2′-*O*-acylation featured in uglas#11 (**4**) requires *cest-1.1*,[20] and 6′-*O*-acylation of *N*-acetylserotonin glucosides requires *cest-4*.[21]

From a metabolomics perspective, the use of the AIF-based screen enabled detection of a large number of nucleobase-derived metabolites, whose identification via traditional chromatography/nuclear magnetic resonance (NMR)-based strategies would not have been feasible, given the enormous complexity of animal metabolomes. The large number of possible methylation and glycosylation positions presented additional challenges. Ultimately, close integration of synthesis with the MS-based structure elucidation process was central to the success of this work. Compound identification thus partly depended on adaption of nucleoside chemistry for gluconucleoside synthesis and was facilitated by the serendipitous discovery of facile 2′-*O*- to 3′-*O*-phosphoryl transesterification, greatly reducing the need for *N*- and *O*-protective groups. This dibenzyl phosphate migration is analogous to well-known acyl migration between adjacent equatorial OH groups in hexoses[24,47,48] or the TBDMS 2′-*O*- to 3′-*O*-migration on cyclodextrins.[49,50]

CONCLUSIONS

Our results show that gluconucleoside production is conserved in nematodes and may motivate a broader reinvestigation of nucleoside metabolism in animals and other phyla. Beyond nematodes, there is building evidence for reuse and further metabolism of nucleoside building blocks in other organisms. For example, the venom of hobo spiders, *Tegenaria agrestis*, contains a collection of sulfated guanosines, including fucosylated derivatives, such as **45**.[51,52] Microbial examples include sinefungin (**46**)[53] from *Streptomyces* and the recently reported human vaginal microbiota-derived tyrocitabine-626 (**47**), featuring an unusual orthoester-phosphate combined with a tyrosine-derived building block (Figure 6e).[54] Moreover, production of the antiviral 3′-deoxy,-3′,4′-didehydro-cytidine triphosphate (ddhCTP, **47**) via the radical SAM enzyme, viperin, provides an intriguing example of a non-canonical nucleoside encoded by mammalian genomes.[55]

Finally, our analyses confirmed the presence of several broadly conserved DNA and RNA modifications in *C. elegans*,[29,56–58] including N^1- and N^2-methylguanosine. These had

previously been assigned only putatively,[29] highlighting a surprising lack of characterization of nucleoside metabolism in model systems, in spite of the discovery opportunities enabled by HRMS-based metabolomics.

Supplementary Material

Refer to Web version on PubMed Central for supplementary material.

ACKNOWLEDGMENTS

Some strains used in this work were provided by the CGC, which is funded by the NIH Office of Research Infrastructure Programs (P40 OD010440). We thank Gary Horvath for technical support and Ivan Keresztes and David Kiemle for assistance with NMR spectroscopy.

Funding

This research was supported in part by the National Institutes of Health (R35GM131877 to F.C.S.) and a Faculty Scholar grant (to F.C.S.) by the Howard Hughes Medical Institute. A.T. is supported by a CIHRI Institute of Aging fellowship.

ABBREVIATIONS

A	adenine
C	cytosine
G	guanine
T	thymine
U	uracil
MA	methyladenine
MG	methylguanine
DMA	dimethyladenine
DMG	dimethylguanine
MTA	5′-methylthioadenosine
[O]-MTA	oxidized 5′-methylthioadenosine
AIF	all-ion fragmentation
BSA	bis(trimethylsilyl)acetamide
Cbz	carboxybenzyl
ddhCTP	3′-deoxy,-3′,4′-didehydro-cytidine triphosphate
CEST	carboxylesterase
ESI$^+$	electrospray ionization positive mode

HPLC−HRMS	high-performance liquid chromatography–high-resolution mass spectrometry
ImOTf	imidazole trifluoromethanesulfonate
mCPBA	3-chloroperoxybenzoic acid
MS^2	tandem mass spectrometry
ms2i6A	2-methylthio-N^6-isopentenyladenine
t6A	N^6-threonylcarbamoyladenine
TBAF	tetrabutylammonium fluoride
TBDMS	*t*-butyldimethylsilyl
TBTU	2-(1*H*-benzotriazole-1-yl)-1,1,3,3-tetramethy-laminium tetrafluoroborate
tRFs	tRNA fragments
UGT	uridine diphosphoglucuronosyltransferase

REFERENCES

(1). Jordheim LP; Durantel D; Zoulim F; Dumontet C Advances in the development of nucleoside and nucleotide analogues for cancer and viral diseases. Nat. Rev. Drug Discovery 2013, 12, 447–464. [PubMed: 23722347]

(2). Damaraju VL; Damaraju S; Young JD; Baldwin SA; Mackey J; Sawyer MB; Cass CE Nucleoside anticancer drugs: the role of nucleoside transporters in resistance to cancer chemotherapy. Oncogene 2003, 22, 7524–7536. [PubMed: 14576856]

(3). Chien M; Anderson TK; Jockusch S; Tao C; Li X; Kumar S; Russo JJ; Kirchdoerfer RN; Ju J Nucleotide Analogues as Inhibitors of SARS-CoV-2 Polymerase, a Key Drug Target for COVID-19. J. Proteome Res 2022, 19, 4690–4697.

(4). Artyukhin AB; Zhang YK; Akagi AE; Panda O; Sternberg PW; Schroeder FC Metabolomic "Dark Matter" Dependent on Peroxisomal β-Oxidation in *Caenorhabditis elegans*. J. Am. Chem. Soc 2018, 140, 2841–2852. [PubMed: 29401383]

(5). Bose N; Ogawa A; von Reuss SH; Yim JJ; Ragsdale EJ; Sommer RJ; Schroeder FC Complex small-molecule architectures regulate phenotypic plasticity in a nematode. Angew. Chem., Int. Ed. Engl 2012, 51, 12438–12443. [PubMed: 23161728]

(6). Curtis BJ; Kim LJ; Wrobel CJJ; Eagan JM; Smith RA; Burch JE; Le HH; Artyukhin AB; Nelson HM; Schroeder FC Identification of Uric Acid Gluconucleoside-Ascaroside Conjugates in *Caenorhabditis elegans* by Combining Synthesis and MicroED. Org. Lett 2020, 22, 6724–6728. [PubMed: 32820938]

(7). Hou B; Lim EK; Higgins GS; Bowles DJ N-glucosylation of cytokinins by glycosyltransferases of *Arabidopsis thaliana*. J. Biol. Chem 2004, 279, 47822–47832. [PubMed: 15342621]

(8). Pokorná E; Hluska T; Galuszka P; Hallmark HT; Dobrev PI; Záveská Drábková L; Filipi T; Holubová K; Plíhal O; Rashotte AM; Filepová R; Malbeck J; Novák O; Spíchal L; Brzobohaty B; Mazura P; Zahajská L; Motyka V Cytokinin N-glucosides: Occurrence, Metabolism and Biological Activities in Plants. Biomolecules 2021, 11, 24.

(9). Moffatt BA; Ashihara H Purine and pyrimidine nucleotide synthesis and metabolism. Arabidopsis Book 2002, 1, No. e0018. [PubMed: 22303196]

(10). Geiger T; Cox J; Mann M Proteomics on an Orbitrap Benchtop Mass Spectrometer Using All-ion Fragmentation. Mol. Cell. Proteomics 2010, 9, 2252–2261. [PubMed: 20610777]

(11). Graca G; Cai Y; Lau CE; Vorkas PA; Lewis MR; Want EJ; Herrington D; Ebbels TMD Automated Annotation of Untargeted All-Ion Fragmentation LC-MS Metabolomics Data with MetaboAnnotatoR. Anal. Chem 2022, 94, 3446–3455. [PubMed: 35180347]

(12). Chaleckis R; Naz S; Meister I; Wheelock CE LC-MS-Based Metabolomics of Biofluids Using All-Ion Fragmentation (AIF) Acquisition. Methods Mol. Biol 2018, 1730, 45–58. [PubMed: 29363064]

(13). Montgomery JA; Thomas HJ 7-Glycosylpurines. I. The synthesis of the anomeric 7-D-ribofuranosyladenines and the identification of the nucleoside from pseudovitamin B1–12. J. Am. Chem. Soc 1965, 87, 5442–5447. [PubMed: 5844821]

(14). Friedmann HC; Fyfe JA Pseudovitamin B 12 biosynthesis. Enzymatic formation of a new adenylic acid, 7-alpha-D-ribofuranosyladenine 5′-phosphate. J. Biol. Chem 1969, 244, 1667–1671. [PubMed: 5780835]

(15). Jones JW; Robins RK; Purine Nucleosides III Methylation Studies of Certain Naturally Occurring Purine Nucleosides. J. Am. Chem. Soc 1963, 85, 193–201.

(16). Niedballa U; Vorbrüggen H A general synthesis of pyrimidine nucleosides. Angew. Chem., Int. Ed. Engl 1970, 9, 461–462. [PubMed: 4988014]

(17). Tranova L; Styskala J Study of the N(7) Regioselective Glycosylation of 6-Chloropurine and 2,6-Dichloropurine with Tin and Titanium Tetrachloride. J. Org. Chem 2021, 86, 13265–13275. [PubMed: 34528791]

(18). Stupp GS; von Reuss SH; Izrayelit Y; Ajredini R; Schroeder FC; Edison AS Chemical detoxification of small molecules by Caenorhabditis elegans. ACS Chem. Biol 2013, 8, 309–313. [PubMed: 23163740]

(19). Wrobel CJJ; Yu J; Rodrigues PR; Ludewig AH; Curtis BJ; Cohen SM; Fox BW; O'Donnell MP; Sternberg PW; Schroeder FC Combinatorial Assembly of Modular Glucosides via Carboxylesterases Regulates C. elegans Starvation Survival. J. Am. Chem. Soc 2021, 143, 14676–14683. [PubMed: 34460264]

(20). Le HH; Wrobel CJ; Cohen SM; Yu J; Park H; Helf MJ; Curtis BJ; Kruempel JC; Rodrigues PR; Hu PJ; Sternberg PW; Schroeder FC Modular metabolite assembly in *Caenorhabditis elegans* depends on carboxylesterases and formation of lysosome-related organelles. Elife 2020, 9, No. e61886. [PubMed: 33063667]

(21). Yu J; Vogt MC; Fox BW; Wrobel CJJ; Fajardo Palomino D; Curtis BJ; Zhang B; Le HH; Tauffenberger A; Hobert O; Schroeder FC Parallel pathways for serotonin biosynthesis and metabolism in C. elegans. Nat. Chem. Biol 2023, 19, 141–150. [PubMed: 36216995]

(22). Hayakawa Y; Kataoka M Facile Synthesis of Oligodeoxyr-ibonucleotides via the Phosphoramidite Method without Nucleoside Base Protection. J. Am. Chem. Soc 1998, 120, 12395–12401.

(23). Ohkubo A; Ezawa Y; Seio K; Sekine M O-selectivity and utility of phosphorylation mediated by phosphite triester intermediates in the N-unprotected phosphoramidite method. J. Am. Chem. Soc 2004, 126, 10884–10896. [PubMed: 15339173]

(24). Patel MK; Davis BG Control of phosphoryl migratory transesterifications allows regioselecive access to sugar phosphates. Org. Lett 2013, 15, 346–349. [PubMed: 23286302]

(25). Sim MM; Kondo H; Wong CH Synthesis of dibenzyl glycosyl phosphites using dibenzyl N,N-diethylphosphoramidite as phosphitylating reagent: an effective route to glycosyl phosphates, nucleotides, and glycosides. J. Am. Chem. Soc 1993, 115, 2260–2267.

(26). Twibanire JD; Grindley TB Efficient and controllably selective preparation of esters using uronium-based coupling agents. Org. Lett 2011, 13, 2988–2991. [PubMed: 21591807]

(27). Twibanire JD; Omran RP; Grindley TB Facile synthesis of a library of Lyme disease glycolipid antigens. Org. Lett 2012, 14, 3909–3911. [PubMed: 22784298]

(28). Dieterich C; Clifton SW; Schuster LN; Chinwalla A; Delehaunty K; Dinkelacker I; Fulton L; Fulton R; Godfrey J; Minx P; Mitreva M; Roeseler W; Tian H; Witte H; Yang SP; Wilson RK; Sommer RJ The *Pristionchus pacificus* genome provides a unique perspective on nematode lifestyle and parasitism. Nat. Genet 2008, 40, 1193–1198. [PubMed: 18806794]

(29). van Delft P; Akay A; Huber SM; Bueschl C; Rudolph KLM; Di Domenico T; Schuhmacher R; Miska EA; Balasubramanian S The Profile and Dynamics of RNA Modifications in Animals. ChemBioChem 2017, 18, 979–984. [PubMed: 28449301]

(30). Burkhardt RN; Artyukhin AB; Aprison EZ; Curtis BJ; Fox BW; Ludewig AH; Palomino DF; Luo J; Chaturbedi A; Panda O; Wrobel CJJ; Baumann V; Portman DS; Lee SS; Ruvinsky I; Schroeder FC Sex-specificity of the C. elegans metabolome. Nat. Commun 2023, 14, 320. [PubMed: 36658169]

(31). Salameh Y; Bejaoui Y; El Hajj N DNA Methylation Biomarkers in Aging and Age-Related Diseases. Front. Genet 2020, 11, 171. [PubMed: 32211026]

(32). Wilkinson GS; Adams DM; Haghani A; Lu AT; Zoller J; Breeze CE; Arnold BD; Ball HC; Carter GG; Cooper LN; Dechmann DKN; Devanna P; Fasel NJ; Galazyuk AV; Gunther L; Hurme E; Jones G; Knornschild M; Lattenkamp EZ; Li CZ; Mayer F; Reinhardt JA; Medellin RA; Nagy M; Pope B; Power ML; Ransome RD; Teeling EC; Vernes SC; Zamora-Mejias D; Zhang J; Faure PA; Greville LJ; Herrera ML; Flores-Martinez JJ; Horvath S DNA methylation predicts age and provides insight into exceptional longevity of bats. Nat. Commun 2021, 12, 1615. [PubMed: 33712580]

(33). Shen H; Lan Y; Zhao Y; Shi Y; Jin J; Xie W The emerging roles of N6-methyladenosine RNA methylation in human cancers. Biomarker Res. 2020, 8, 24.

(34). Stewart KR; Veselovska L; Kelsey G Establishment and functions of DNA methylation in the germline. Epigenomics 2016, 8, 1399–1413. [PubMed: 27659720]

(35). Baugh LR; Hu PJ Starvation Responses Throughout the Caenorhabditiselegans Life Cycle. Genetics 2020, 216, 837–878. [PubMed: 33268389]

(36). Tauffenberger A; Fiumelli H; Almustafa S; Magistretti PJ Lactate and pyruvate promote oxidative stress resistance through hormetic ROS signaling. Cell Death Dis. 2019, 10, 653. [PubMed: 31506428]

(37). Huang Z; Xie N; Illes P; Di Virgilio F; Ulrich H; Semyanov A; Verkhratsky A; Sperlagh B; Yu SG; Huang C; Tang Y From purines to purinergic signalling: molecular functions and human diseases. Signal Transduction Targeted Ther. 2021, 6, 162.

(38). Thompson DM; Lu C; Green PJ; Parker R tRNA cleavage is a conserved response to oxidative stress in eukaryotes. RNA 2008, 14, 2095–2103. [PubMed: 18719243]

(39). Sulthana S; Basturea GN; Deutscher MP Elucidation of pathways of ribosomal RNA degradation: an essential role for RNase E. RNA 2016, 22, 1163–1171. [PubMed: 27298395]

(40). Houseley J; Tollervey D The Many Pathways of RNA Degradation. Cell 2009, 136, 763–776. [PubMed: 19239894]

(41). Saikia M; Hatzoglou M The Many Virtues of tRNA-derived Stress-induced RNAs (tiRNAs): Discovering Novel Mechanisms of Stress Response and Effect on Human Health. J. Biol. Chem 2015, 290, 29761–29768. [PubMed: 26463210]

(42). Yu M; Lu B; Zhang J; Ding J; Liu P; Lu Y tRNA-derived RNA fragments in cancer: current status and future perspectives. J. Hematol. Oncol 2020, 13, 121. [PubMed: 32887641]

(43). Magee R; Rigoutsos I On the expanding roles of tRNA fragments in modulating cell behavior. Nucleic Acids Res. 2020, 48, 9433–9448. [PubMed: 32890397]

(44). Smehilova M; Dobruskova J; Novak O; Takac T; Galuszka P Cytokinin-Specific Glycosyltransferases Possess Different Roles in Cytokinin Homeostasis Maintenance. Front. Plant Sci 2016, 7, 1264. [PubMed: 27602043]

(45). Li P; Lei K; Li Y; He X; Wang S; Liu R; Ji L; Hou B Identification and characterization of the first cytokinin glycosyltransferase from rice. Rice 2019, 12, 19. [PubMed: 30923923]

(46). Faghih N; Bhar S; Zhou Y; Dar AR; Mai K; Bailey LS; Basso KB; Butcher RA A Large Family of Enzymes Responsible for the Modular Architecture of Nematode Pheromones. J. Am. Chem. Soc 2020, 142, 13645–13650. [PubMed: 32702987]

(47). Lassfolk R; Pedrón M; Tejero T; Merino P; Wärnå J; Leino R Acyl Group Migration in Pyranosides as Studied by Experimental and Computational Methods. Chem. – Eur. J 2022, 28, No. e202200499.

(48). Dimakos V; Taylor MS Site-Selective Functionalization of Hydroxyl Groups in Carbohydrate Derivatives. Chem. Rev 2018, 118, 11457–11517. [PubMed: 30507165]

(49). Ashton PR; Boyd SE; Gattuso G; Hartwell EY; Koeniger R; Spencer N; Stoddart JF A Novel Approach to the Synthesis of Some Chemically-Modified Cyclodextrins. J. Org. Chem 1995, 60, 3898–3903.

(50). Teranishi K; Ueno F Mechanism of 2-O3-O silyl migration in cyclomaltohexaose (α-cyclodextrin). Tetrahedron Lett. 2003, 44, 4843–4848.

(51). Taggi AE; Meinwald J; Schroeder FC A new approach to natural products discovery exemplified by the identification of sulfated nucleosides in spider venom. J. Am. Chem. Soc 2004, 126, 10364–10369. [PubMed: 15315451]

(52). Schroeder FC; Taggi AE; Gronquist M; Malik RU; Grant JB; Eisner T; Meinwald J NMR-spectroscopic screening of spider venom reveals sulfated nucleosides as major components for the brown recluse and related species. Proc. Natl. Acad. Sci. U. S. A 2008, 105, 14283–14287. [PubMed: 18794518]

(53). Hamil RL; Hoehn MM A9145, a new adenine-containing antifungal antibiotic. I. Discovery and isolation. J. Antibiot 1973, 26, 463–465.

(54). Patel JR; Oh J; Wang S; Crawford JM; Isaacs FJ Crosskingdom expression of synthetic genetic elements promotes discovery of metabolites in the human microbiome. Cell 2022, 185, 1487–1505.e14. [PubMed: 35366417]

(55). Gizzi AS; Grove TL; Arnold JJ; Jose J; Jangra RK; Garforth SJ; Du Q; Cahill SM; Dulyaninova NG; Love JD; Chandran K; Bresnick AR; Cameron CE; Almo SC A naturally occurring antiviral ribonucleotide encoded by the human genome. Nature 2018, 558, 610–614. [PubMed: 29925952]

(56). Greer EL; Blanco MA; Gu L; Sendinc E; Liu J; Aristizabal-Corrales D; Hsu CH; Aravind L; He C; Shi Y DNA Methylation on N^6-Adenine in *C. elegans*. Cell 2015, 161, 868–878. [PubMed: 25936839]

(57). Yokoyama W; Hirota K; Wan H; Sumi N; Miyata M; Araoi S; Nomura N; Kako K; Fukamizu A rRNA adenine methylation requires T07A9.8 gene as rram-1 in *Caenorhabditis elegans*. J. Biochem 2018, 163, 465–474. [PubMed: 29385568]

(58). Zhu C; Yan Q; Weng C; Hou X; Mao H; Liu D; Feng X; Guang S Erroneous ribosomal RNAs promote the generation of antisense ribosomal siRNA. Proc. Natl. Acad. Sci. U. S. A 2018, 115, 10082–10087. [PubMed: 30224484]

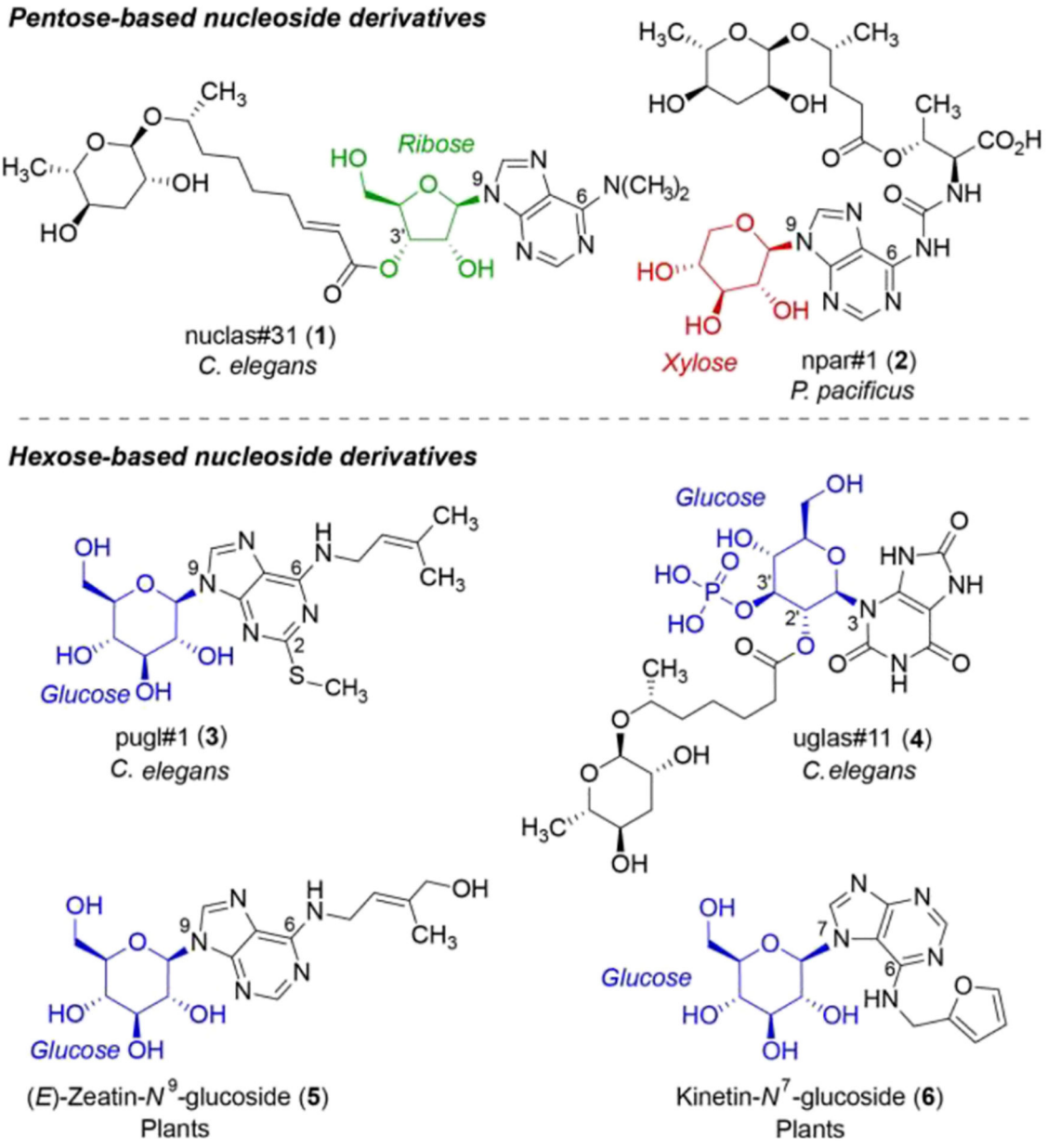

Figure 1.

Examples of nucleoside-related metabolites in nematodes and plants. Whereas nuclas#31 (**1**) is based on canonical dimethyladenine riboside, other recently described nucleoside derivatives integrate other sugars, the pentose xylose in npar#1 (**2**) and glucose in pugl#1 (**3**) and uglas#11 (**4**). Related cytokinin glucosides (**5** and **6**) found in plants.

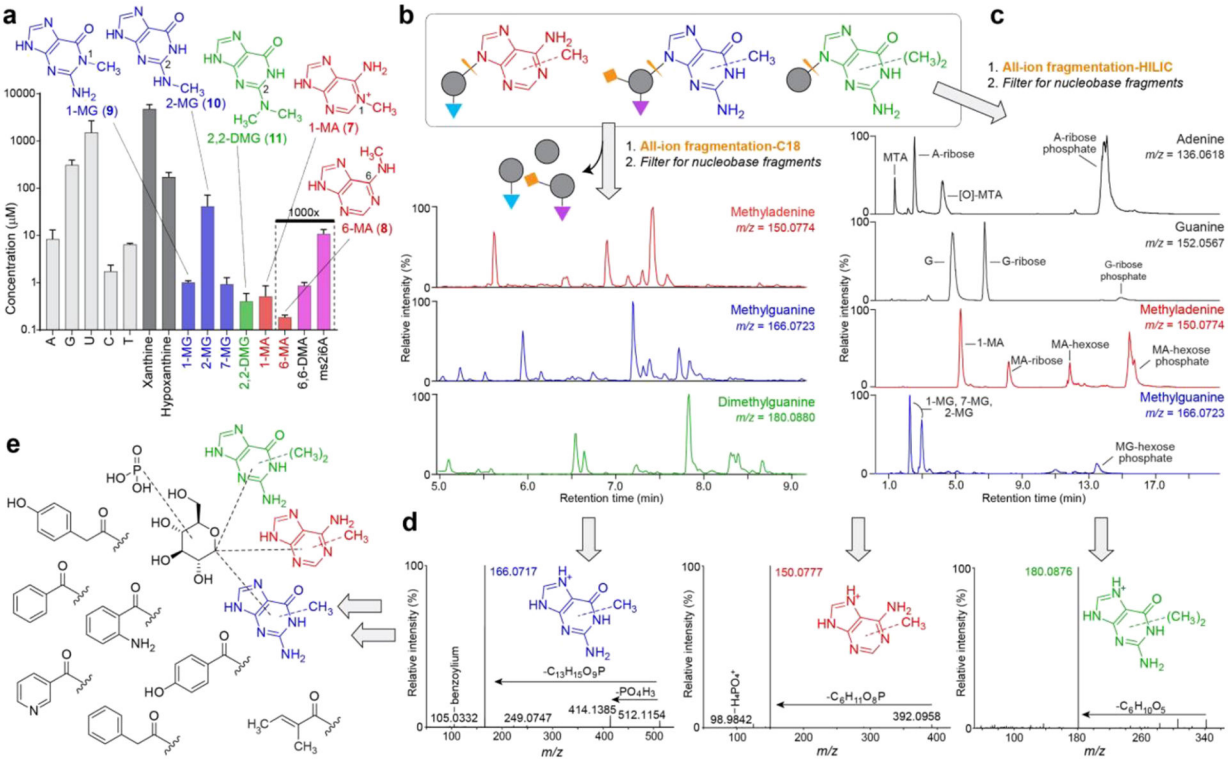

Figure 2.

Profiling the *C. elegans* metabolome for nucleoside derivatives. (a) Nucleobase profile obtained from *endo*-metabolome samples. In addition, small amounts of t6A were detected but could not be quantified. (b, c) HPLC−HRMS analyses of the *endo*-metabolome using AIF and reversed-phase C18 (Method A, b) and HILIC chromatography (Method D, c) reveal diverse methylpurine glycosides. (d) MS^2 of methylpurine-containing metabolites in ESI^+ mode. (e) MS^2 analysis reveals a family of putative acylated methylpurine glycosides, integrating diverse moieties from amino acid metabolism. A, adenine; C, cytosine; G, guanine; T, thymine; U, uracil; MA, methyladenine; MG, methylguanine; DMA, dimethyladenine; DMG, dimethylguanine; t6A, N^6-threonylcarbamoyladenine; ms2i6A, 2-methylthio-N^6-isopentenyladenine; MTA, 5′-methylthioadenosine; [O]-MTA, oxidized MTA.

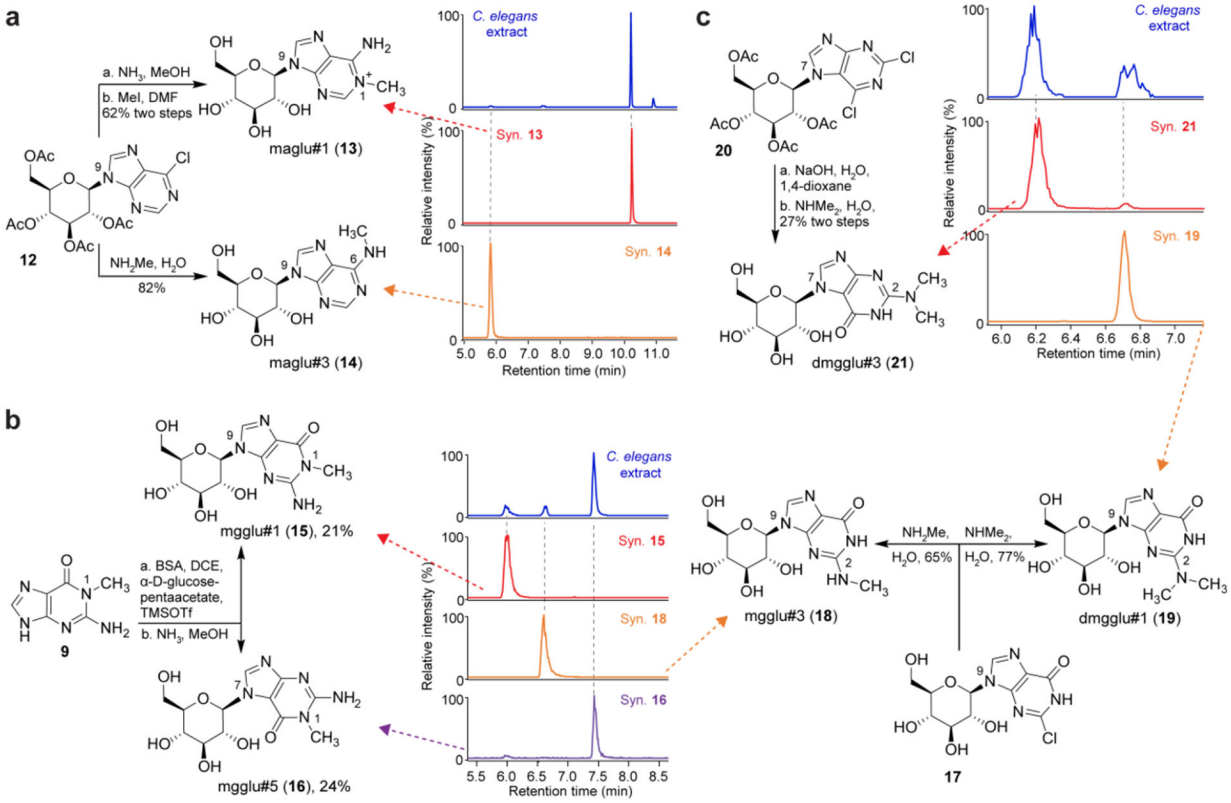

Figure 3.

Identification of glucosylated methylpurines. Syntheses and retention time comparison via HILIC−MS (ESI^+, Method C) of metabolome samples and synthetic standards of (a) methyladenine, (b) methylguanine, and (c) dimethylguanine. Syn., synthetic. In panel (c), the *C. elegans* extract shows several peaks at 6.7–6.9 min, the first of which corresponds to dmgglu#1 (**19**).

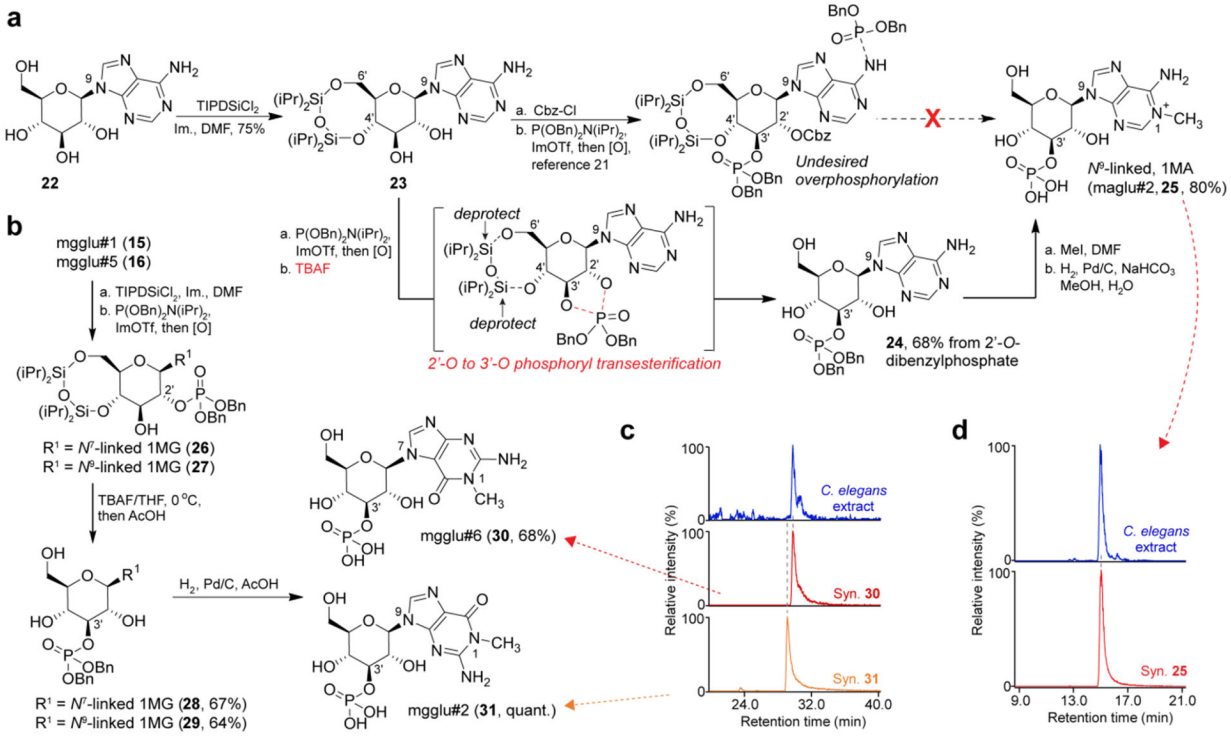

Figure 4.

Phosphorylated gluconucleosides. (a) Initial plan (top) for the synthesis of 3′-*O*-phosphorylated methyladenine glucoside (maglu#2, **25**) and revised approach (bottom) via one-pot desilylation/phosphoryl transesterification. (b) Analogous synthesis of methylguanine derivatives mglu#6 (**30**) and mglu#2 (**31**) using 2′-*O*-phosphates (**26** and **27**) derived from mglu#5 (**16**) and mglu#1 (**15**). Extracted-ion chromatograms (ESI^+) comparing the *C. elegans endo*-metabolome and synthetic standards of methylguanine glucosides mglu#2 (**31**) and mglu#6 (**30**) (c, HILIC-Method E) and methyladenine glucoside maglu#2 (**25**) (d, HILIC-Method D).

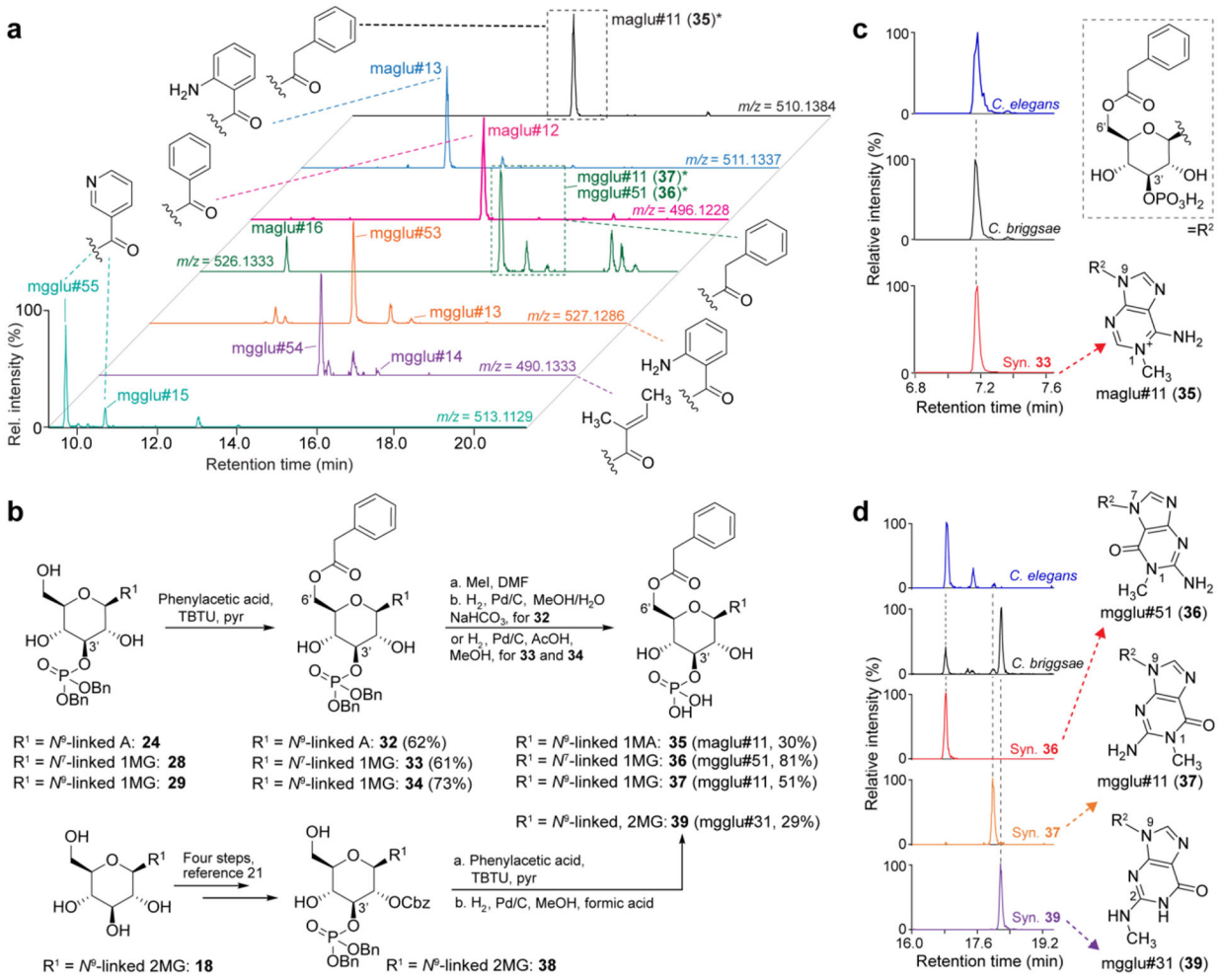

Figure 5.

Synthesis and identification of *O*-acylated gluconucleosides. (a) Extracted-ion chromatograms (ESI^+, C18-Method B) for acylated gluconucleosides in *C. elegans* containing methylpurines, as inferred from MS^2 spectra (Figure 2). Metabolites whose structures were confirmed in this study are marked by an asterisk (*). Other assignments are putative and based solely on MS^2. See Figures S17 and S18 for structures. (b) Synthetic routes to 6′-*O*-phenylacetylated glucosides (**35**–**37**), starting from protected 3′-*O*-phosphates (**32**–**34**). A separate route utilizing 2′-*O*-Cbz protection afforded 6′-*O*-phenylacetylated N^2-methylguanine (mgglu#31, **39**). (c, d) Extracted-ion chromatograms (ESI^+) comparing *C. elegans*, *C. briggsae*, and synthetic standards of maglu#11 (c, C18-Method A) and several mgglu#-family metabolites (d, C18, Method B).

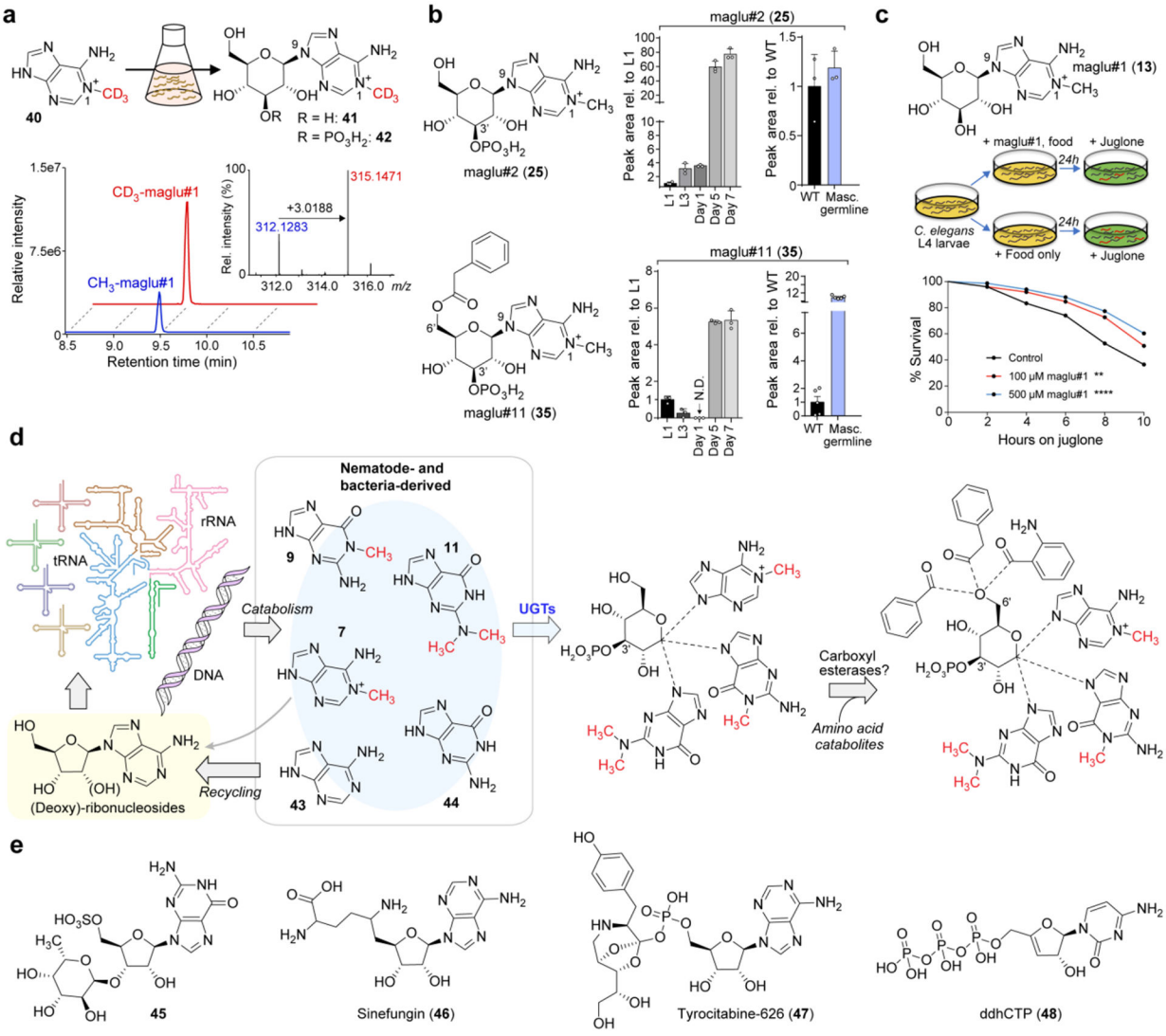

Figure 6.

Origin and bioactivity of gluconucleosides. (a) Supplementation of stable-isotope labeled (CD_3) and non-labeled (CH_3) N^1-methyladenine. Extracted-ion chromatograms (ESI^+, HILIC-Method C) reveal extensive incorporation of the isotope label into maglu#1 (**13**). (b) Gluconucleoside production increases with age in adult animals. The shown trend for maglu#2 (**25**) is representative of non-acylated gluconucleosides and their phosphates. Phenylacetylated gluconucleosides, e.g., maglu#11 (**35**), are specifically associated with the male germline (also see Figure S30 and data tables in ref 30). (c) maglu#1 (**13**) increases survival under oxidative stress. Animals were treated with maglu#1 (**13**) 24 h prior to exposure to oxidative stress-inducing juglone. Data are from three individual experiments with 50 animals/condition each. (d) Proposed biogenesis of methylpurine-derived glucosides in nematodes. (e) Structures of unusual nucleoside derivatives, including a sulfated guanosine (**45**) from *Tegenaria agrestis*, the microbial metabolites sinefungin (**46**) and tyrocitabine (**47**), and the mammalian metabolite ddhCTP (**48**).